Available online at www.sciencedirect.com
ScienceDirect
Journal of Catalysis 254 (2008) 64–70
JOURNAL OF CATALYSIS
www.elsevier.com/locate/jcat

# Synthesis and catalytic activity of Ti-MCM-41 nanoparticles with highly active titanium sites

Kaifeng Lin [a], Paolo P. Pescarmona [a,*], Hans Vandepitte [a], Duoduo Liang [b], Gustaaf Van Tendeloo [b], Pierre A. Jacobs [a]

[a] *COK, K.U. Leuven, Kasteelpark Arenberg 23-bus 2461, 3001 Heverlee, Belgium*
[b] *EMAT, UA, Groenenborglaan 171, 2020 Antwerpen, Belgium*

Received 13 September 2007; revised 28 November 2007; accepted 28 November 2007

**Abstract**

Ti-MCM-41 nanoparticles 80–160 nm in diameter (Ti-MCM-41 NP) were successfully prepared by a dilute solution route in sodium hydroxide medium at ambient temperature. Ti-MCM-41 NP were characterized by X-ray diffraction, nitrogen adsorption/desorption isotherms, SEM, TEM, FT-IR, and UV–vis spectroscopy. The characterization results showed the existence of highly ordered hexagonal mesoporous structure and tetrahedral Ti species in Ti-MCM-41 NP. In the epoxidation of cyclohexene with aqueous $H_2O_2$, Ti-MCM-41 NP displayed higher conversion and initial reaction rate than a Ti-MCM-41 sample with normal particle size (Ti-MCM-41 LP). Diffusion of the reactants was accelerated and the accessibility to the catalytic Ti species was enhanced in the shorter channels in Ti-MCM-41 NP samples. Ti-MCM-41 NP showed much higher selectivity for cyclohexene oxide compared with Ti-MCM-41 LP, suggesting reduced hydrolysis of cyclohexene oxide with water in the former case. The increased selectivity for cyclohexene oxide can be attributed to the lower concentration of residual surface silanols in Ti-MCM-41 NP and the shorter residence time of epoxide in the shorter mesoporous channels. Ti-MCM-41 NP also appears to be a suitable catalyst in the epoxidation of a bulky substrate, like cholesterol, with *tert*-butyl hydroperoxide.


*Keywords:* Ti-MCM-41 nanoparticles; Dilute solution route; Short mesoporous channels; Epoxidation of cyclohexene; Cholesterol

## 1. Introduction

Titanium-containing mesoporous silicates have attracted much attention in the past 10 years because of their potential as selective oxidation catalysts for bulky organic substrates. Since the preparation of titanium-containing mesoporous silicates using cetyltrimethylammonium bromide or dodecylamine as the surfactant in an alkaline media was reported [1,2], numerous attempts have been made to prepare and apply such materials as catalysts for various bulky molecules [3–14]. Several reactions, including the oxygenation of benzene, phenol, di-*tert*-butyl phenol, olefins, and thioethers, have been studied over titanium-containing mesoporous silicates. However, the activity and selectivity on the materials reported to date are lower than those on microporous titanosilicate zeolites, at least for the oxygenation of relatively small organic substrates [15]. Low hydrophobicity, low Ti/Si molar ratio, and large particle size of these titanium-containing mesoporous silicates have been proposed as the three main reasons for the reduced activity [16].

Efforts at improving the catalytic properties of such solids have focused on enhancing hydrophobicity and increasing the Ti/Si molar ratio [17–23]. To date, no attempt to improve the catalytic performance of titanium-containing mesoporous silicates by decreasing their particle size has been reported, even though it is commonly accepted that large particle sizes in titanium-containing mesoporous silicates a cause of for their low activities. Small particle size also is important for obtaining higher activities with titanium-substituted zeolite catalysts. In the hydroxylation of phenol with hydrogen peroxide, a decrease in the crystal size of TS-1 leads to enhanced activity [24,25].

* Corresponding author. Fax: +32 16 321998.
*E-mail address:* paolo.pescarmona@biw.kuleuven.be (P.P. Pescarmona).

0021-9517/$ – see front matter 
doi:10.1016/j.jcat.2007.11.017

In this article, we describe the synthesis of nanoparticles of Ti-MCM-41 with short mesoporous channels and highly active titanium species. First, we used these materials to catalyze the epoxidation of cyclohexene with aqueous $H_2O_2$, which is frequently used as a test reaction for the catalytic evaluation of titanosilicate catalysts. Second, we performed the oxidation of cholesterol with *tert*-butyl hydroperoxide to evaluate the potential of Ti-MCM-41 nanoparticles in epoxidation of bulky substrates.

## 2. Experimental

### 2.1. Preparation of the catalysts

Ti-MCM-41 nanoparticles (Ti-MCM-41 NP) were prepared from titanosilicate gels using a very low surfactant concentration, according to a method comparable to that reported for the preparation of MCM-41 nanoparticles [26]. In this method, known as the diluted solution route, first 3.5 mL of 2 M NaOH aqueous solution was added to a mixture of 480 mL of distilled water and 1.0 g of cetyltrimethylammonium bromide (CTAB, Acros) under stirring. The concentration of CTAB in the solution was $2.1 \times 10^{-3}$ g/mL. Then titanium(IV) isopropoxide (TIP, Aldrich) and tetraethyl orthosilicate (TEOS, Acros) were slowly added to the homogeneous solution under stirring at 700–900 rpm, which yielded a white gel (molar ratio of $H_2O$/NaOH/CTAB/TEOS/TIP = 1197/0.31/0.125/1/0.025). After being stirred for 2 h at ambient temperature, the resulting solid (Ti-MCM-41 NP) was filtered, washed with 1500 mL of distilled water on a Büchner funnel, dried at 60 °C, and calcined in air at 550 °C for 6 h (at a heating rate of 1 °C/min).

For comparison, Ti-MCM-41 with larger particles (Ti-MCM-41 LP) was synthesized as described previously [17] in an ammonia aqueous solution. The molar ratio of $H_2O$/$NH_4OH$/CTAB/TEOS/TIP was 62/3.3/0.1/1/0.025, with a CTAB concentration in the solution of $2.7 \times 10^{-2}$ g/mL.

### 2.2. Characterization

X-ray diffraction (XRD) patterns were obtained with a STOE STADI P transmission diffractometer using Cu$K\alpha$ radiation. FT-IR spectra of the samples were recorded on a Nicolet 730 FT-IR spectrometer using self-supported wafers of 6.7 mg/cm$^2$. UV–vis spectra were measured with a Varian Cary 5 spectrophotometer equipped with a diffuse-reflectance accessory in the region of 200–800 nm. The isotherms of nitrogen were measured at the temperature of liquid nitrogen using a Micromeritics TriStar 3000. The pore-size distribution was calculated using the Barrett–Joyner–Halenda (BJH) model. Scanning electron microscopy (SEM) images were obtained on a Philips XL30 FEG, and transmission electron microscopy (TEM) images were obtained on a Philips CM 20. Si elemental analysis was carried out by a chemical method, and Ti elemental analysis was performed by inductively coupled plasma-optical emission spectroscopy (ICP-OES) using a Perkin-Elmer Optima 3000DV. The presence of Na was monitored by energy-dispersive X-ray spectroscopy (EDX) on a Philips XL30 FEG.

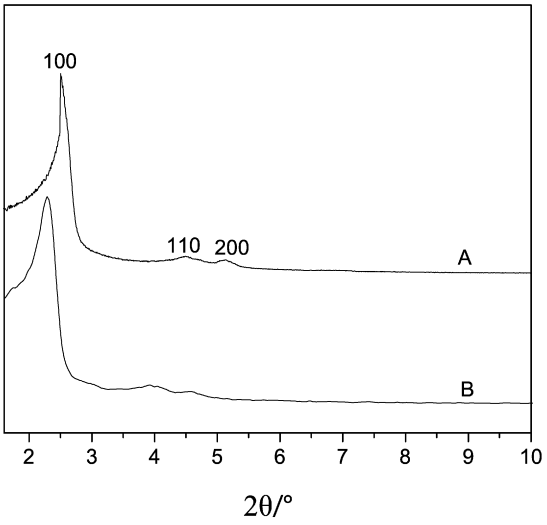


Fig. 1. X-ray diffraction pattern of Ti-MCM-41 NP (A) and Ti-MCM-41 LP (B).

The amount of $H_2O_2$ decomposed in $H_2O$ and $O_2$ during the catalytic tests was determined by titration of the reaction solution with a 0.1 M solution of $Ce(SO_4)_2$, prepared by dissolving $Ce(SO_4)_2{\cdot}4H_2O$ (50.0 mmol) in $H_2SO_4$ (28 mL) and bidistilled $H_2O$ (28 mL) and diluted to a total volume of 500 mL with $H_2O$. The reaction solution was separated from the solid catalyst by centrifugation. Then 0.5 mL of this solution was diluted with $H_2O$ (18 mL) and a 7 vol% aqueous solution of $H_2SO_4$ (2 mL). The colorless solution thus obtained was titrated with the 0.1 M $Ce^{IV}$ solution until it turned yellow ($2Ce^{4+} + H_2O_2 \rightarrow 2Ce^{3+} + 2H^+ + O_2$).

### 2.3. Catalytic reactions

The epoxidation of cyclohexene with an aqueous solution of $H_2O_2$ was carried out in a glass vial under vigorous stirring. In a typical run, 4.5 mmol of cyclohexene, 4.5 mL of solvent, and 30 mg of catalyst were mixed in the vial and heated to the desired temperature. Aqueous $H_2O_2$ (2.25 mmol, 50 wt%) was added to the mixture to start the reaction. The catalysts were separated by centrifugation and the products were analyzed with a gas chromatograph (Agilent 6850) using a HP-1 capillary column of 30 m and a FID detector.

The epoxidation of cholesterol with *tertiary* butyl hydroperoxide (TBHP) was carried out in a batch reactor at 90 °C for 24 h. Here, 1.92 mmol of cholesterol, 1.18 mmol of TBHP (~5 M in *n*-decane), and 50 mg of catalyst were mixed in 50 mL of toluene. After the reaction, the catalyst was separated from the mother liquid, the products were silylated with *N*-methyl-*N*-(trimethylsilyl) trifluoroacetamide (200 μL of MSTFA to 1 mL of reaction mixture) and analyzed using gas chromatography (GC) and GC-mass spectroscopy (Agilent 68901).

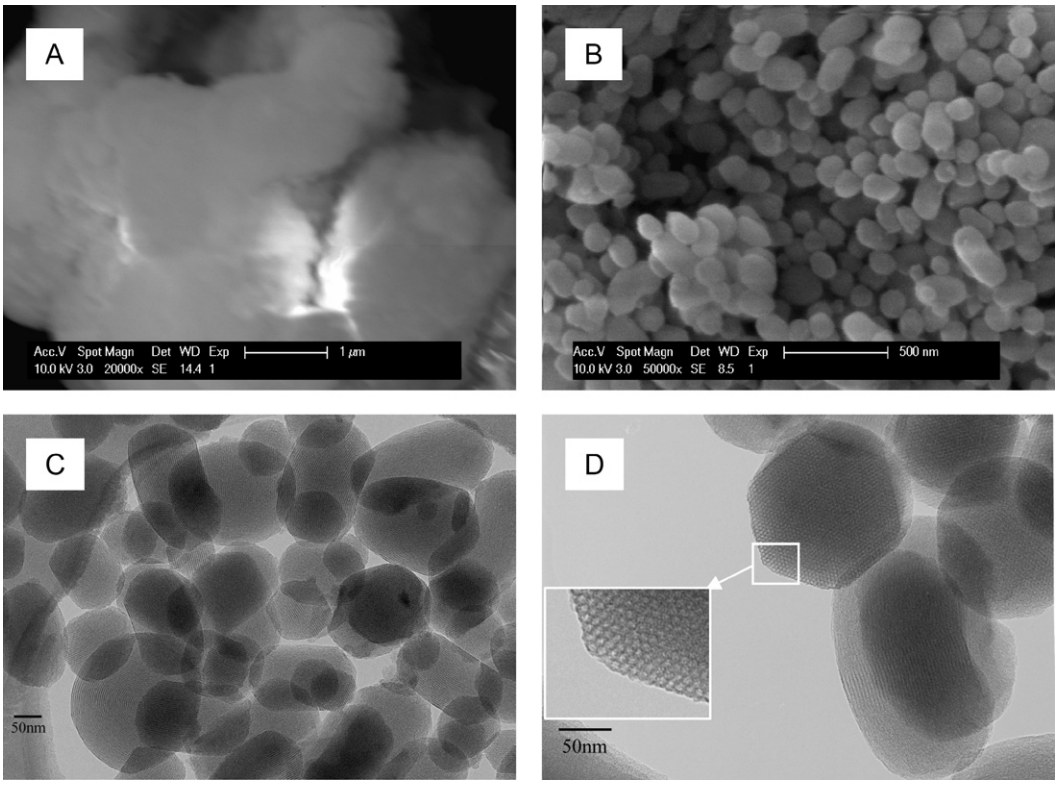


Fig. 2. SEM images of Ti-MCM-41 LP (A) and Ti-MCM-41 NP (B) and TEM images of Ti-MCM-41 NP (C, D).

## 3. Results and discussion

### 3.1. X-ray diffraction

Fig. 1 shows the XRD patterns of calcined Ti-MCM-41 NP and Ti-MCM-41 LP. Although the $d_{100}$ values of Ti-MCM-41 NP and Ti-MCM-41 LP are different, both samples give three diffraction peaks, indexed as (100), (110), and (200) reflections, indicating that Ti-MCM-41 NP has an ordered hexagonal mesostructure similar to that of Ti-MCM-41 LP. This long-range order is in agreement with that found for MCM-41 nanoparticles prepared using the diluted solution route [26,27].

### 3.2. SEM and TEM images

The morphology and structure of the obtained Ti-MCM-41 NP are clearly revealed by the SEM and TEM images. The morphology of Ti-MCM-41 LP consists of irregular bulky particles (Fig. 2A). In contrast, SEM images of Ti-MCM-41 NP from the diluted solution route (Fig. 2B) show nanosized (elongated) spherical particles ranging in size from 80 to 160 nm. TEM images of Ti-MCM-41 NP (Figs. 2C and 2D) show the existence of highly ordered hexagonal arrays and one-dimensional mesoporous parallel channels within the nanoparticles. The TEM results confirm that Ti-MCM-41 NP is a pure phase and that every nanoparticle has short, ordered mesoporous channels.

The formation of MCM-41 nanoparticles depends on the length of silicate rodlike micelles, which in turn is determined by the type of base used; $NH_4OH$ media favors longer micelles, whereas NaOH media favors shorter micelles [26]. The TEM results show that the NaOH medium played the same role in the formation of Ti-MCM-41 NP. Although the synthesis was carried out in a Na-rich solution, negligible amounts of Na were incorporated into the Ti-MCM-41 NP, as proved by EDX analysis.

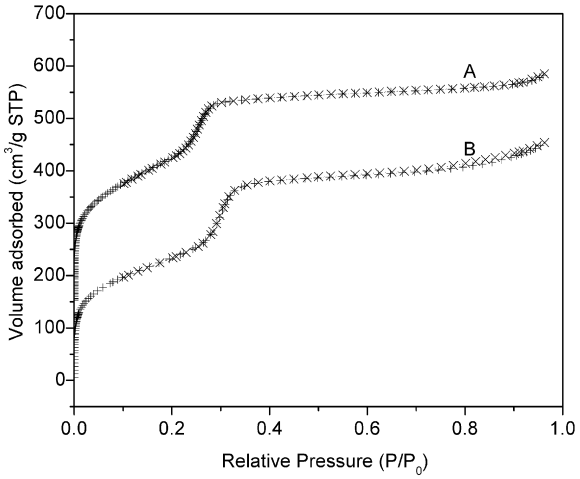


Fig. 3. Nitrogen adsorption (+)/desorption (×) isotherms of Ti-MCM-41 NP (A) and Ti-MCM-41 LP (B). Isotherm A is offset by 150 $cm^3/g$ along the vertical axis for clarity.

### 3.3. Nitrogen adsorption/desorption isotherms

$N_2$ adsorption/desorption isotherms of calcined Ti-MCM-41 NP and Ti-MCM-41 LP gave typical type-IV isotherms with a sharp inflection at relative $P/P_0 > 0.3$ (Fig. 3). This is character-

Table 1
Textural properties of calcined Ti-MCM-41 NP and Ti-MCM-41 LP[a]

| | Ti-MCM-41 NP | Ti-MCM-41 LP |
|---|---|---|
| $d_{100}$ (nm) | 3.5 | 3.9 |
| Average pore size (nm) | 2.4 | 2.7 |
| Wall thickness (nm)[b] | 1.6 | 1.8 |
| Pore volume ($cm^3/g$) | 0.58 | 0.54 |
| Surface area ($m^2/g$) | 1012.5 | 847.3 |

[a] Pore-size distributions and pore volumes were determined from $N_2$ adsorption isotherms at 77 K.
[b] The wall thickness was calculated as: $a_0$-pore size ($a_0 = 2 \times d(100)/3^{1/2}$).

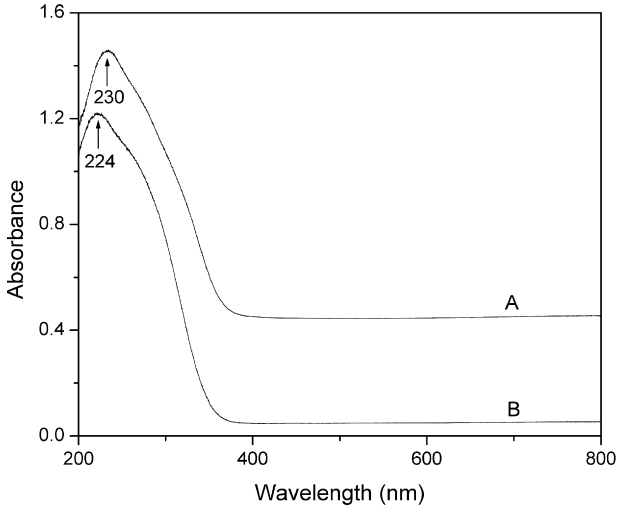


Fig. 4. UV–vis spectra of Ti-MCM-41 NP (A) and Ti-MCM-41 LP (B). Spectrum A is offset by 0.4 along the vertical axis for clarity.

istic of capillary condensation, which points to the uniformity of the mesopore size distribution. Table 1 lists the textural properties of Ti-MCM-41 NP and Ti-MCM-41 LP. It is noteworthy that the BET surface area of Ti-MCM-41 NP from dilute solution route (1012.5 $m^2/g$) is much higher than that of Ti-MCM-41 LP (847.3 $m^2/g$). This is attributed to the smaller particle size of Ti-MCM-41 NP, because Ti-MCM-41 NP and Ti-MCM-41 LP had similar pore sizes, pore volume, and wall thickness (Table 1).

### 3.4. UV–vis spectroscopy

A correlation between the position of the UV–vis absorption band and the coordination of titanium species in silicates is commonly accepted [28–30]. Fig. 4 shows the UV–vis spectra of calcined Ti-MCM-41 NP and Ti-MCM-41 LP, which have similar Si/Ti ratios (45.2 and 47.4, respectively). Both samples showed a very similar band at 224–230 nm attributed to distorted tetrahedral Ti species in the mesoporous structure, which is in good agreement with other titanium-containing MCM-41 samples [16]. The absence of a band at 330 nm indicates the absence of anatase in the samples. The shoulder at 270 nm likely corresponds to partially polymerized hexa-coordinated Ti species [5], originating from the high titanium content in both samples. All characterization results indicate that Ti-MCM-41 NP prepared by the diluted solution route and Ti-MCM-41 LP have comparable structural and textural properties, except for particle size and surface area.

Table 2
Catalytic activities in the epoxidation of cyclohexene over Ti-MCM-41 NP and Ti-MCM-41 LP catalysts in different solvents[a]

| | Si/Ti (molar) | Solvent | Conversion[b] (%) | TON[c] |
|---|---|---|---|---|
| Ti-MCM-41 LP | 47.4 | $CH_3CN$[d] | 29.1 | 127.1 |
| Ti-MCM-41 NP | 45.2 | $CH_3CN$[d] | 36.1 | 150.5 |
| Ti-MCM-41 LP | 47.4 | $CH_3OH$[e] | 13.2 | 57.7 |
| Ti-MCM-41 NP | 45.2 | $CH_3OH$[e] | 25.6 | 106.7 |

[a] Reaction conditions: 4.5 mL of solvent, 4.5 mmol of cyclohexene, 2.25 mmol of $H_2O_2$ (50 wt% in water), 30 mg of catalyst.
[b] The conversion is based on cyclohexene.
[c] Turnover number in mol (mol of Ti)$^{-1}$.
[d] Reaction temperature 70 °C, reaction time 2 h.
[e] Reaction temperature 40 °C, reaction time 4 h.

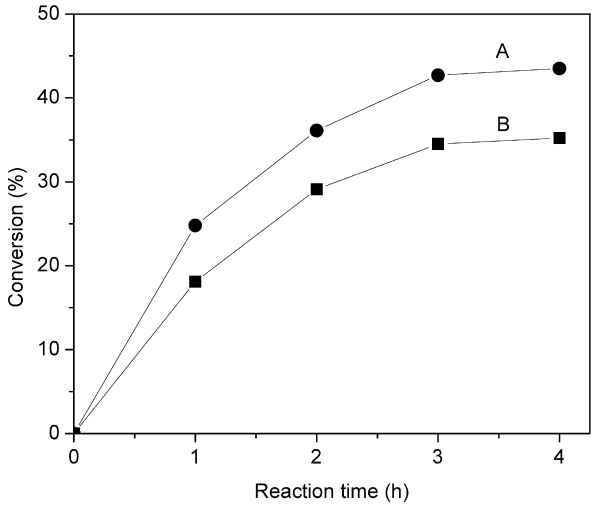


Fig. 5. Catalytic activities in the epoxidation of cyclohexene with $H_2O_2$ as a function of reaction time over Ti-MCM-41 NP (A) and Ti-MCM-41 LP (B). For the reaction conditions, see Table 2.

### 3.5. Catalytic reactions

Table 2 presents the catalytic activities of Ti-MCM-41 NP and Ti-MCM-41 LP in the epoxidation of cyclohexene with aqueous $H_2O_2$ in different solvents. In both acetonitrile and methanol, Ti-MCM-41 NP displayed higher conversion of cyclohexene and TON than Ti-MCM-41 LP. Furthermore, Ti-MCM-41 NP displayed high efficiency in the use of hydrogen peroxide for the epoxidation reaction (85–90%) when acetonitrile was the solvent. Based on the characterization results, the increased catalytic activity with Ti-MCM-41 NP should be attributed to the decrease in the particle size of Ti-MCM-41 to nanometer scale, which enhances the accessibility of the reactants to the catalytic Ti species in the shorter channels of Ti-MCM-41 NP.

Fig. 5 shows the catalytic activity of Ti-MCM-41 NP and Ti-MCM-41 LP in the epoxidation of cyclohexene in acetonitrile as a function of reaction time. Ti-MCM-41 NP exhibited

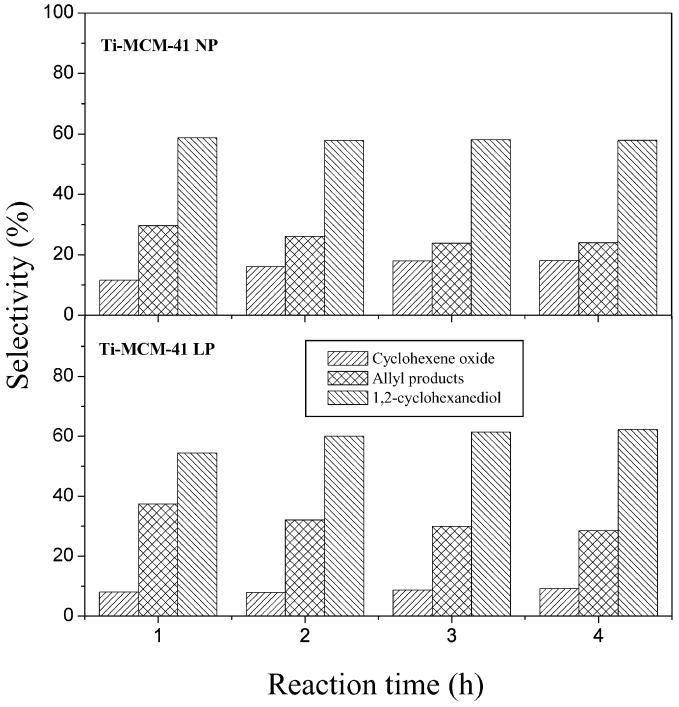


Fig. 6. The selectivities for products as a function of the reaction time over Ti-MCM-41 NP and Ti-MCM-41 LP. For the reaction conditions, see Table 2.

not only higher conversion of cyclohexene after 4 h, but also a higher initial reaction rate than Ti-MCM-41 LP.

Over the two catalysts tested, four different products of the oxidation of cyclohexene with aqueous $H_2O_2$ were detected: cyclohexene epoxide (CHE), 1,2-cyclohexanediol (CHD), 2-cyclohexene-1-ol (CH-OH), and 2-cyclohexene-1-one (CH-ONE). Whereas cyclohexene oxide is generated by the heterolytic epoxidation of the cyclohexene double bond, 1,2-cyclohexanediol is formed by catalytic hydrolysis of the epoxide ring of cyclohexene oxide in the presence of strong acid sites. Allylic oxidation products, CH-OH and CH-ONE, can form via homolytic radical pathways. Fig. 6 shows the selectivity toward the various products of the epoxidation of cyclohexene in acetonitrile as a function of reaction time with Ti-MCM-41 NP and Ti-MCM-41 LP. The yield of cyclohexene epoxide after 4 h with Ti-MCM-41 NP was almost double of that with Ti-MCM-41 LP, and Ti-MCM-41 NP showed a much higher selectivity for cyclohexene epoxide than Ti-MCM-41 LP at any reaction time. The average selectivity ratio between CHE and CHD at different reaction times with Ti-MCM-41 NP was approximately twice that with Ti-MCM-41 LP. These results indicate that the hydrolysis of cyclohexene epoxide to 1,2-cyclohexanediol is reduced in Ti-MCM-41 NP. Considering the structure of Ti-MCM-41 NP, a possible reason for this is

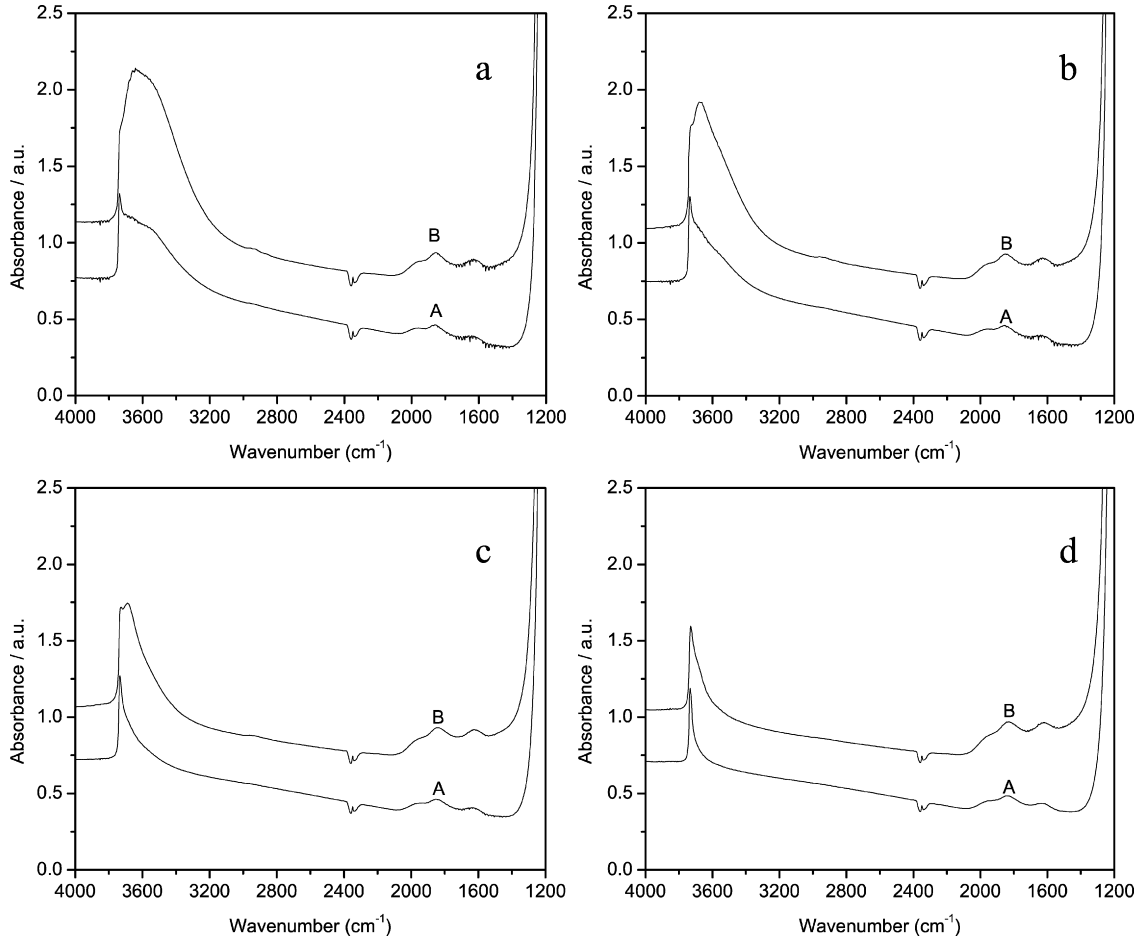


Fig. 7. FT-IR spectra of Ti-MCM-41 NP (A) and Ti-MCM-41 LP (B) pre-treated in dry, flowing He at (a) 200, (b) 300, (c) 400, and (d) 550 °C. Spectrum B is offset by 0.5 along the vertical axis for clarity.

the shorter residence time of cyclohexene epoxide in the pores of the catalyst, which would reduce the possibility of further reaction of CHE. Another explanation involves the difference in silanol concentration in the two titanosilicates. It has been proposed that $H_2O_2$ causes the formation of acid sites in the residual surface silanols hydrogen bonded to titanium hydroperoxide surface species in titanosilicates [31]. These sites can play an important role in the hydrolysis of cyclohexene epoxide. Consequently, the silanol concentration in the two catalysts was studied by FT-IR spectroscopy. Fig. 7 shows the FT-IR spectra in the vibration region of 1200–4000 $cm^{-1}$ of wafers (~6.7 $mg/cm^2$) of Ti-MCM-41 NP and Ti-MCM-41 LP samples precalcined at 550 °C, reexposed to the laboratory atmosphere, and treated in dry flowing helium at different temperatures. The absence of significant intensity variations in the water deformation region (1600–1700 $cm^{-1}$) on changing the wafer degassing temperature indicates that parallel changes in the OH-stretching region (3800–3300 $cm^{-1}$) should be attributed to changes in relative concentration of free and hydrogen-bonded silanols [32]. Comparing the OH band absorption intensity of Ti-MCM-41 NP and Ti-MCM-41 LP, it follows that the amount of free and hydrogen-bonded silanols was much lower in Ti-MCM-41 NP. The lower number of silanols leads to a decrease in surface acidity, and, therefore, to less hydrolysis of cyclohexene epoxide. As a result, the epoxide selectivity should be enhanced, which is in good agreement with the catalytic results (Fig. 6). The IR band intensity and width both decreased gradually with increasing temperature, indicating removal of a considerable number of hydrogen-bonded silanols, with siloxane bridges formed at higher temperature. When the temperature reached 550 °C, only a sharp absorption band at 3740 $cm^{-1}$ remained. Comparison of the respective peak intensities shows that the Ti-MCM-41 NP sample had a significantly reduced number of residual silanols. It also follows that H-bonded silanols were reversibly formed on exposure of precalcined samples to air moisture.

To evaluate the samples' recyclability potential, Ti-MCM-41 NP was washed and reused in several 4-h catalytic cycles. Fig. 8a shows the results of the repeated use of Ti-MCM-41 NP after four room temperature washings with ethanol. The cyclohexene conversion gradually decreased during subsequent runs. The deactivation can be attributed to gradual leaching of Ti, as observed for the classically prepared Ti-MCM-41 [33] and/or to the deposition of reaction residue not soluble in ethanol. The ratio of epoxidation to ring-opening selectivity slowly decreased as well. Thus, repeated use also seems to affect the number of residual acid sites, which appear to be more susceptible to removal than the Ti sites. The regeneration of Ti-MCM-41 NP via intermediate calcination at 550 °C for 2 h shows results comparable to those from recycling by washing (Fig. 8b). With this procedure, the possibility that the gradual decrease in cyclohexene conversion is due to heavy product deposition can be excluded, because adsorbed byproducts that hinder the coordination of the reagents to the active centers would be removed during the intermediate calcinations. The deactivation might be due to the aggregation of Ti-MCM-41 NP particles and/or enhanced removal of Ti species from their original location

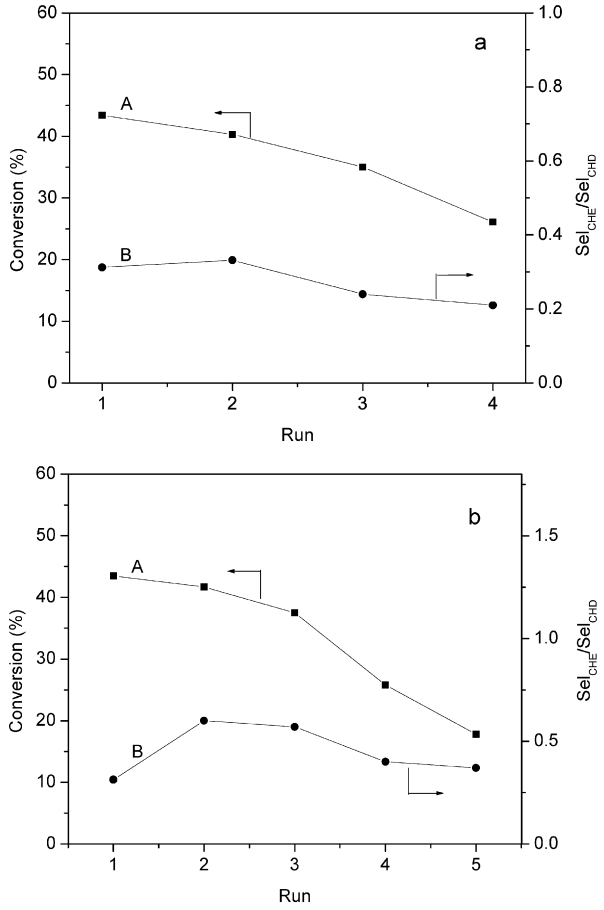


Fig. 8. Results of repeated use of Ti-MCM-41 NP in the epoxidation of cyclohexene by washing (a) and calcination (b) approaches: (A) conversion and (B) selectivity ratio for CHE and CHD. The reaction conditions are the same as those in Table 2.

Table 3
Catalytic activities in the epoxidation of cholesterol with TBHP over Ti-MCM-41 NP and Ti-MCM-41 catalysts[a]

| | Si/Ti (molar) | Yield of epoxide[b] (%) | TON (on epoxide basis) |
|---|---|---|---|
| Ti-MCM-41 NP | 45.2 | 5.0 | 5.3 |
| Ti-MCM-41 LP | 47.4 | 4.0 | 4.4 |
| Ti-MCM-41[c] | 10 | 25.4 | ~4.4 |

[a] Reaction conditions: 1.92 mmol cholesterol, 1.18 mmol TBHP (~5 M in *n*-decane), 50 mg of catalyst, 50 mL of toluene, 50 mg of catalyst, 90 °C, 24 h.
[b] The yield is based on cholesterol. Epoxide: 5α,6α-epoxycholesterol.
[c] From Ref. [11].

during calcination. It should be noted that the activities of Ti-MCM-41 NP after 3 successive runs (35% and 37.5%; Fig. 8, a and b) are compatible to that of freshly prepared Ti-MCM-41 LP (35.2%).

Table 3 presents the catalytic performance of epoxidation of cholesterol with TBHP over Ti-MCM-41 NP and Ti-MCM-41 LP catalysts. It is well known that TS-1 is inactive due to the inaccessibility of the small micropores of TS-1 to a bulky molecule, like cholesterol. On the other hand, Ti-MCM-41 LP and Ti-MCM-41 NP were both active for this reaction, with 5α, 6α-epoxycholesterol yields of 4.0 and 5.0%. No ketocholesterol,

hydroxycholesterol, or other oxygenated byproducts were observed. This result demonstrates that Ti-MCM-NP is a suitable catalyst for the oxidation of bulky molecules as well.

## 4. Conclusion

Ti-MCM-41 nanoparticles (Ti-MCM-41 NP) of 80–160 nm diameter were successfully prepared at ambient temperature from a diluted solution route in sodium hydroxide medium. Characterization of Ti-MCM-41 NP indicate the existence of highly ordered hexagonal arrays and one-dimensional mesoporous parallel channels in the nanoparticles. Ti-MCM-41 NP displayed higher conversions, TON values, and initial reaction rate than Ti-MCM-41 LP in the epoxidation of cyclohexene with aqueous $H_2O_2$, indicating that shorter mesoporous channels in the nanosized particles of Ti-MCM-41 NP play an important role in accelerating the diffusion rate of reactant/product molecules in the pores. Furthermore, Ti-MCM-41 NP gave much higher selectivity for cyclohexene oxide than Ti-MCM-41 LP at any reaction time, due to reduced hydrolysis of cyclohexene oxide with water. Ti-MCM-41 NP could be recycled to an acceptable extent after regeneration through washing or calcination approaches. The catalytic results in the epoxidation of cholesterol indicate that Ti-MCM-NP is a suitable catalyst for the oxidation of bulky molecules as well.

## Acknowledgments

K.L. and H.V. are grateful for a Center of Excellence grant (CECAT) from K.U. Leuven and an SBO grant (BIPOM) from the IWT. P.P.P. acknowledges the Fund for Scientific Research (FWO) for a postdoctoral fellowship. The authors also acknowledge support from the following research programs: CECAT, BIPOM, IAP, GOA, and IDECAT.

## References

[1] A. Corma, M.T. Navarro, J. Pérez Pariente, Chem. Commun. (1994) 147.
[2] P.T. Tanev, M. Chibwe, T.J. Pinnavaia, Nature 368 (1994) 321.
[3] O. Franke, J. Rathousky, G. Schulz-Ekloff, J. Starek, A. Zukal, Stud. Surf. Sci. Catal. 84 (1994) 77.
[4] S. Gontier, A. Tuel, J. Catal. 157 (1995) 124.
[5] G. Schulz-Ekloff, J. Rathousky, A. Zukal, Div. Pet. Chem. 40 (2) (1995) 221.
[6] T. Blasco, A. Corma, M.T. Navarro, J. Pérez Pariente, J. Catal. 156 (1995) 65.
[7] M. Morey, A. Davidson, G.D. Stucky, Microporous Mater. 6 (1996) 99.
[8] I.F. Vankelecom, N.M. Moens, K.A. Vercruysse, A.L. Karen, R.F. Parton, P.A. Jacobs, Stud. Surf. Sci. Catal. 108 (1997) 437.
[9] K.A. Koyano, T. Tatsumi, Microporous Mater. 10 (1997) 259.
[10] D. Trong On, M.P. Kapoor, P.N. Joshi, L. Bonneviot, S. Kaliaguine, Catal. Lett. 44 (1997) 171.
[11] K.A. Vercruysse, D.M. Klingeleers, T. Colling, P.A. Jacobs, Stud. Surf. Sci. Catal. 117 (1998) 469.
[12] B.L. Newalkar, J. Olanrewaju, S. Komarneni, Chem. Mater. 13 (2001) 552.
[13] S.C. Laha, R. Kumar, Microporous Mesoporous Mater. 53 (2002) 163.
[14] W.H. Zhang, J.Q. Lu, B. Han, M.J. Li, J.H. Xiu, P.L. Ying, C. Li, Chem. Mater. 14 (2002) 3413.
[15] B. Notari, in: D.D. Eley, W.O. Haag, B.C. Gates (Eds.), Advances in Catalysis, vol. 41, Academic Press, San Diego, 1996, p. 253.
[16] A. Bhaumik, T. Tatsumi, J. Catal. 189 (2000) 31.
[17] K. Lin, L. Wang, F.Y. Meng, Z. Sun, Q. Yang, Y. Cui, D. Jiang, F.-S. Xiao, J. Catal. 235 (2005) 423.
[18] B. Notari, Adv. Catal. 41 (1996) 253.
[19] A. Corma, M. Domine, J.A. Gaono, J.L. Jorda, M.T. Navarro, F. Rey, J. Pérez Pariente, J. Tsuji, B. McCulloch, L.T. Nemeth, J. Chem. Soc. Chem. Commun. (1998) 2211.
[20] T. Tatsumi, K.A. Koyano, N. Igarashi, Chem. Commun. (1998) 325.
[21] G. Perego, R. Millini, G. Bellussi, in: H.G. Karge, J. Weitkamp (Eds.), in: Molecular Sieves Science and Technology, vol. 1, Springer, Berlin, 1998, p. 187.
[22] Z. Shan, E. Gianotti, J.C. Jansen, J.A. Peters, L. Marchese, T. Maschmeyer, Chem. Eur. J. 7 (2001) 1437.
[23] M. Ramakrishna Prasad, G. Madhavi, A. Ramachander Rao, S.J. Kulkarni, K.V. Raghavan, J. Porous Mater. 13 (2006) 81.
[24] A.J.H.P. van der Pol, A.J. Verduyn, J.H.C. van Hooff, Appl. Catal. A Gen. 92 (1992) 113.
[25] U. Wilkenhöner, G. Langhendries, F. van Laar, G.V. Baron, D.W. Gammon, P.A. Jacobs, E. van Steen, J. Catal. 203 (2001) 201.
[26] Q. Cai, Z.S. Luo, W.Q. Pang, Y.W. Fan, X.H. Chen, F.Z. Cui, Chem. Mater. 13 (2001) 258.
[27] R.I. Nooney, D. Thirunavukkarasu, Y. Chen, R. Josephs, A.E. Ostafin, Chem. Mater. 14 (2002) 4721.
[28] A. Zecchina, G. Spoto, S. Bordiga, A. Ferrero, G. Petrini, M. Padovan, G. Leofanti, Stud. Surf. Sci. Catal. 69 (1991) 251.
[29] G. Ricchiardi, A. Damin, S. Bordiga, C. Lamberti, G. Spano, F. Rivetti, A. Zecchina, J. Am. Chem. Soc. 121 (2001) 11409.
[30] S. Bordiga, S. Coluccia, C. Lamberti, L. Marchese, A. Zecchina, F. Boscherini, F. Buffa, F. Genoni, G. Leofanti, G. Petrini, G. Vlaic, J. Phys. Chem. 98 (1994) 4125.
[31] Y. Goa, P. Wu, T. Tatsumi, J. Phys. Chem. B 108 (2004) 8401.
[32] R.R. Sever, R. Alcala, J.A. Dumesic, T.W. Root, Microporous Mesoporous Mater. 66 (2003) 53.
[33] J.M. Fraile, J.I. García, J.A. Mayoral, E. Vispe, D.R. Brown, M. Naderi, Chem. Commun. (2001) 1510.